

# On the Large-Scale Structure of the Universe as given by the Voronoi Diagrams

L. Zaninetti<sup>1</sup>

Dipartimento di Fisica Generale,  
Via Pietro Giuria 1  
10125 Torino, Italy

Received .....; accepted .....

**Abstract** The size distributions of 2D and 3D Voronoi cells and of cells of  $V_p(2,3)$ ,—2D cut of 3D Voronoi diagram—are explored, with the single-parameter (re-scaled) gamma distribution playing a central role in the analytical fitting. Observational evidence for a cellular universe is briefly reviewed. A simulated  $V_p(2,3)$  map with galaxies lying on the cell boundaries is constructed to compare, as regards general appearance, with the observed CFA map of galaxies and voids, the parameters of the simulation being so chosen as to reproduce the largest observed void size.

**Key words:** surveys ; galaxies :clusters: general ; (Cosmology:) large-scale structure of Universe

## 1 INTRODUCTION

The applications of the Voronoi diagrams (see Voronoi (1908)) in astrophysics started with Kiang (1966) where the size distribution in 1D as given by random seeds was theoretically deduced in a rigorous way. Kiang (1966) also derived , performing a Monte Carlo experiment, the area distribution in 2D and volume distribution in 3D. The idea that area and volume distributions follow a gamma-variate with argument 4 and 6 respectively was later reported as "Kiang's conjecture", see Okabe et al. (1992). The application of the Voronoi diagrams to the distribution of galaxies started with Icke & van de Weygaert (1987), where a sequential clustering process was adopted in order to insert the initial seeds. Later on Pierre (1990) introduced a general algorithm for simulating one-dimensional lines of sight through a cellular universe . The large microwave background

★ E-mail: zaninetti@ph.unito.it

temperature anisotropies over angular scales up to one degree were calculated using a Voronoi model for large-scale structure formation in Barrow & Coles (1990) and Coles (1991).

The possibility to explain the CFA slices using a fractal distribution of seeds and inserting the galaxies on the faces of the irregular polyhedron was explored by Zaninetti (1991) .

A detailed Monte Carlo simulation of pencil beam-like redshift surveys was carried out by Subba Rao & Szalay (1992): they found that the probability of finding regularity varies from 3 to 15 percent depending on the details of the models.

Another Monte Carlo study was carried out by van de Weygaert & Babul (1994) where three different distributions of nuclei were adopted in order to perform extensive statistical analysis of several geometrical aspects of three dimensional Voronoi tessellation. A new way of partitioning the space into cells characterised by the shape of rhombic dodecahedron has been introduced in Kiang (2003) ; the application is done to the CfA catalogue and to the IRAS/PSCz catalogue Kiang et al. (2004). The void hierarchy approach has been introduced in Sheth & van de Weygaert (2004) and it explains how large-scale structures are function of two parameters, one of which reflects the dynamics of void formation, and the other the formation of collapsed objects.

From the point of view of the astronomical observations a few papers that point toward the cellular structure of the universe are now briefly reviewed. On analysing the data from four distinct surveys at the north and south Galactic poles Broadhurst et al. (1990) found an apparent regularity in the galaxy distribution with a characteristic scale of 128 Mpc. The astronomers that analysed the maps of the galaxy distribution up to  $cz=15000$  Km/s , see for example de Lapparent et al. (1988) and Geller & Huchra (1989), found large coherent structures: the largest void found having a diameter of 5000 km/s.

Great advances in the observational data , see Folkes et al. (1999) , Ratcliffe et al. (1996) and Shectman et al. (1996), brought the limits of the observations at  $cz=60000$  Km/s and confirmed the existence of voids in the distribution of galaxies.

The distribution of clusters in rich super-clusters is not isotropic: it is periodic along a cubic lattice approximately aligned with the super-galactic coordinates, see for example Saar et al. (2002).

The Voronoi diagrams are also used to process the astronomical data , see El-Ad & Piran (1997) and Ramella et al. (2001) . As an example Ramella et al. (2001) implemented a Voronoi Galaxy Cluster Finder that uses galaxy positions and magnitudes to find clusters and determine their main features: size, richness and contrast above the background.

The starting point is to consider a series of explosions that start at the same time in a homogeneous space. The shells connected with the explosions meet on a 3D network given by the nested irregular polyhedron. From an astrophysical point of view this network

can be realized by a set of primordial explosions, see Charlton & Schramm (1986) and Zaninetti & Ferraro (1990), described by the Sedov solution in the adiabatic phase:

$$R(t) = \left( \frac{25}{4} \frac{E t^2}{\pi \rho} \right)^{1/5} = 12.49 Mpc \left( \frac{E_{64} t_9^2}{n_{-7}} \right)^{1/5} , \quad (1)$$

where  $t$  represents the time ,  $E$  is the energy injected in the explosion ,  $\rho$  is the density of matter ,  $\rho = nm$  ,  $n$  is number of particles per unit volume ,  $m=1.4m_H$  ,  $m_H$  is the mass of the hydrogen ,  $t_9 = \frac{t}{10^9 yr}$  ,  $E_{64} = \frac{E}{10^{64} erg}$  and  $n_{-7} = \frac{n}{10^{-7} \text{particles cm}^{-3}}$  .

The already cited works leave the following questions unanswered or partially answered.

Is the "Kiang's conjecture" applicable in 2D and 3D environment with physical parameters near to those of the galaxies ?

What is the probability density function that characterises the two-dimensional sectional area connected with 3D Voronoi diagrams ?

Can the averaged area connected with the voids in the distribution of galaxies visible on the CFA2 slices be guessed from the theory ?

Can the number of theoretical voids in the distribution of galaxies in a sphere of radius equal to that of the CFA2 slices be deduced theoretically ?

In order to answer these questions the coefficient of the gamma-variate that characterises the area-distribution of a 2D Voronoi diagram and the volume-distribution in 3D were derived in § 2.5 and in § 3.3 respectively.

The coefficient of the gamma-variate that characterises the sectional area of a 3D Voronoi diagram as well some characteristics of the voids in the distribution of galaxies were derived in § 3.1.

The observed large scale structures of galaxies are classified as CFA slices , LCRS slices or pencil beam surveys : they are simulated in § 4.

The number of seeds necessary to produce a theoretical framework comparable to the observed one was computed in § 4.1.1 .

## 2 THE PRELIMINARIES

The type of adopted lattice , the importance of setting properly the boundary conditions, the type of seeds that generates the polygons/polyhedron , the concept of unitarian area and volume and a first two dimensional scan are now introduced.

### 2.1 The adopted lattice

Our method considers a 2D and a 3D lattice made of  $pixels^2$  and  $pixels^3$  points : present in this lattice are  $N_s$  seeds generated according to a random process. All the computations are usually performed on this mathematical lattice; the conversion to the physical lattice is obtained by multiplying the unit by  $\delta = \frac{side}{pixels-1}$  , where *side* is the length of the square/cube expressed in the physical unit adopted.

## 2.2 Boundary conditions

In order to minimise boundary effects introduced by those polygons/polyhedron that cross the square/cubic boundary, we amplify the area/cube in which the seeds are inserted by a factor *amplify*. Therefore the  $N$  seeds are inserted in an area/volume that is  $pixels^2 \times amplify$  or  $pixels^3 \times amplify$ , which is bigger than the box over which we perform the scanning; *amplify* is generally taken to be equal to 1.2. This procedure inserts periodic boundary conditions to our square/cube. The number of seeds that fall in the area/cube is  $N_s$  with  $N_s < N$ . In order to avoid computing incomplete area/volumes we select the cells that do not intersect the square/cubic boundary. This is obtained by selecting the cells that belong to seeds which are comprised in an area/volume that is *select* times smaller than  $pixels^2$  or  $pixels^3$ ; of course *select* is smaller than one and varies between 0.1 and 0.5.

## 2.3 The seeds

The points are generated independently on the X and Y axis in 2D ( adding the Z axis in 3D ) through a subroutine that returns a pseudo-random real number taken from a uniform distribution between 0 and 1. For practical purposes we used the subroutine RAN1 as described in Press et al. (1992).

## 2.4 The adopted units

In order to deal with quantities of the order of one we divide the obtained area/volume in units of  $pixels^2/pixels^3$  by the expected unitarian area/volume,  $u_A$  and  $u_V$  respectively

$$\begin{aligned} u_A &= pixels^2 \times amplify / N \\ u_V &= pixels^3 \times amplify / N \quad . \end{aligned}$$

This operation represents a first normalisation. The expected unitarian quantities can also be expressed in physical units,  $u_A^p$  and  $u_V^p$

$$\begin{aligned} u_A^p &= side^2 \times amplify / N \\ u_V^p &= side^3 \times amplify / N \quad . \end{aligned}$$

Special attention should be paid when the area is computed like a cut of a 3D network; this case is named  $V_p(2,3)$ , see Sec.3.1. The unitarian area  $u_{A(2,3)}$  is expected to be

$$u_{A(2,3)} = u_V^{2/3} \quad , \quad (2)$$

and the physical counterpart

$$u_{A(2,3)}^p = (u_V^p)^{2/3} \quad . \quad (3)$$

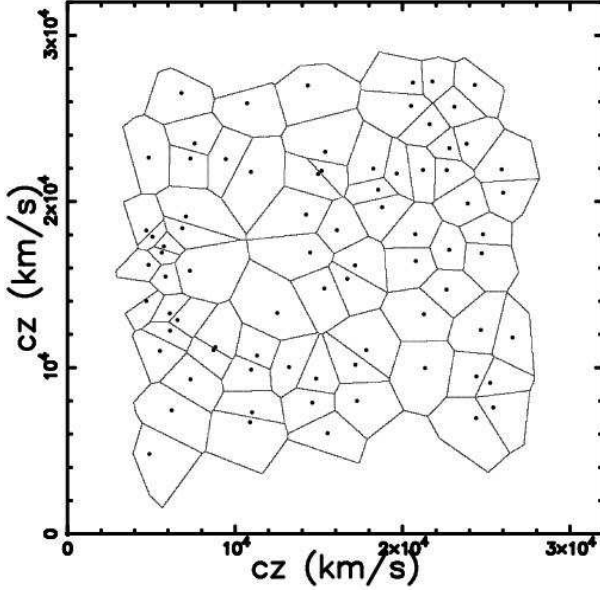


**Fig. 1** The Voronoi-diagram in 2D when random seeds are used. The parameters are  $pixels = 800$  ,  $N = 180$  ,  $amplify = 1.2$  ,  $side = 2 \times 16000$  Km/sec ,  $select = 0.5$

## 2.5 The two dimensional scan

A lattice made of  $(pixel)^2$  points is considered and a typical run using the seeds as given by a random process is visualised in Figure 1. Once the histogram of the area is obtained, we can fit it , following Kiang (1966), with the following one parameter probability density function , in the following pdf:

$$H(x; c) = \frac{c}{\Gamma(c)} (cx)^{c-1} \exp(-cx) \quad , \quad (4)$$

where  $0 \leq x < \infty$  ,  $c > 0$  and  $\Gamma(c)$  is the gamma function with argument  $c$ . This pdf is characterised by  $\mu=1$  and  $\sigma^2=1/c$ . The value of  $c$  is obtained from the method of the matching moments

$$c = \frac{1}{\sigma^2} = \frac{n-1}{\sum_{i=1}^n (x_i - 1)^2} \quad . \quad (5)$$

The data should be normalised in order to have  $\bar{x} = 1$ . The frequency histogram and the relative best fit through the gamma-variate are plotted in Figure 2 . The captions of Figure 2 report also the following quantities expressed in normalised area units (see formula (2))  $\bar{A}$  ,  $A_{max}$  ,  $A_{min}$  , respectively the averaged, the maximum and the minimum of the area-sample and  $\chi^2$  , that represents the goodness of fit.

The value of  $c$  in the case of random seeds is connected with the "Kiang's conjecture" that in 2D means  $c=4$  ; the numerical evaluations give similar values , here  $c = 4.38$  is found.

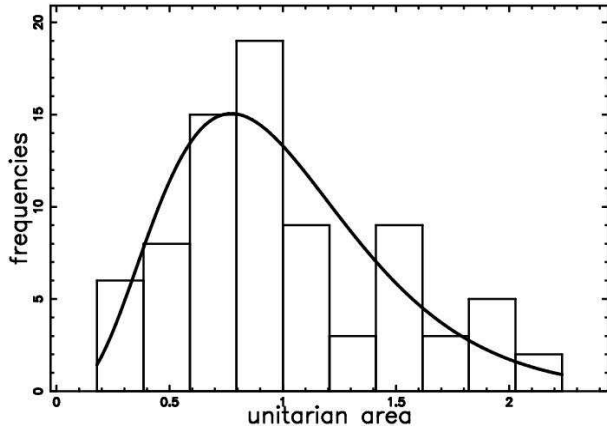


**Fig. 2** Histogram (step-diagram) of area distribution in 2D with a superposition of the fitting line (the gamma-variate); input parameters as in Figure 1,  $c=4.38$ , number of bins =10 ,  $\chi^2=12.67$  ,  $\bar{A} = 0.98$  ,  $A_{max} = 2.19$  ,  $A_{min} = 0.17$  .

### 3 THE 3D CASE

In order to make a comparison with the astronomical observations the tessellation in  $\mathfrak{R}^3$  is firstly analysed through a planar section and the distribution of volume is numerically derived.

#### 3.1 The 2D cut

We now work on a 3D lattice  $L_{k,m,n}$  of pixels<sup>3</sup> elements . Given a section of the cube (characterised , for example, by  $k = \frac{pixel}{2}$ ) the various  $V_i$  (the volume belonging to the seed  $i$ ) may or may not cross the little cubes belonging to the two dimensional lattice .

Following the nomenclature introduced by Okabe et al. (1992) we can call the intersection between a plane and the cube previously described as  $V_p(2,3)$ . A typical result of this 2D sectional operation in the x-y plane can be visualised in Figure 3 , the frequency histogram and the relative best fit through a gamma-variate pdf of the  $V_p(2,3)$  distribution are reported in Figure 4 together with the derived value of  $c$ . Following the hypothesis that the galaxies are distributed on the faces of the irregular polyhedra the network of Figure 3 represents the spatial coordinates where the galaxies are. The thick edges of Figure 3 represent the intersection between the slice and a face ; we remember that the area of intersection increases with  $cz$ .

Due to the great importance that the properties of the sample  $V_p(2,3)$  could have in the astrophysical applications we derived three samples (all crossing the center) of  $V_p(2,3)$  on the x-y , x-z and y-z plane. This allow us to find the average value of the sample properties and their error, see captions of Figure 4.

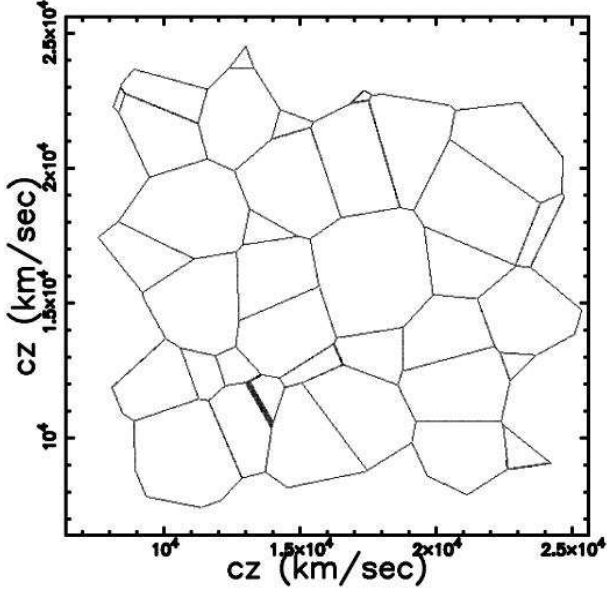


**Fig. 3** Portion of the Voronoi-diagram  $V_p(2,3)$  when random seeds are used; cut on the x-y plane . The parameters are  $pixels = 800$  ,  $N = 1900$  ,  $side = 2 \times 16000$  Km/sec ,  $amplify = 1.2$  and  $select = 0.1$  .

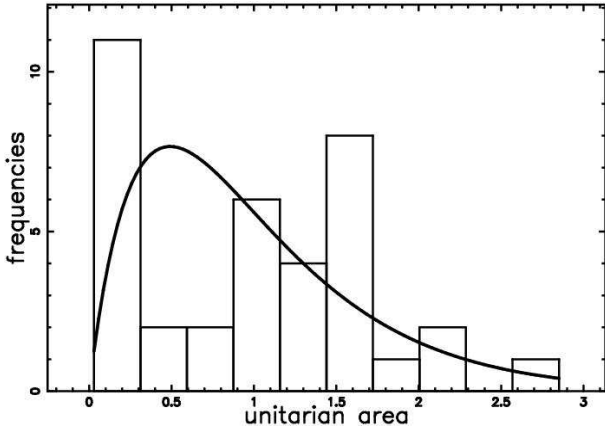


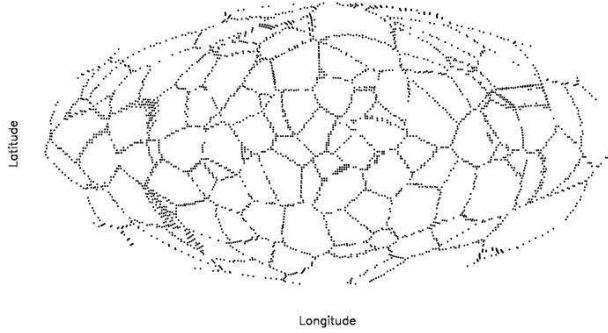
**Fig. 4** Histogram (step-diagram) of  $V_p(2,3)$  distribution on an x-y plane with a superposition of the fitting line (the gamma-variate); parameters as in Figure 3,  $c=1.99 \pm 0.22$ , number of bin =10 ,  $\chi^2=23.09$  ,  $\bar{A} = 0.78 \pm 0.06$  ,  $A_{max} = 2.12 \pm 0.26$  ,  $A_{min} = 0.02 \pm 0.01$  .

The mathematical theory of the expected values of characteristics of a typical cell in 1-dimensional sectional Poisson Voronoi diagram, see Okabe et al. (1992) , gives

$$\bar{A} = 0.68\lambda^{-2/3} , \quad (6)$$

**Table 1** The probability to have  $n$ -edges in  $V_p(2, 3)$ .

seeds \ $n$	3	4	5	6	7	8	9
Okabe et al. (1992)	0.063	0.13	0.2	0.22	0.18	0.11	0.05
random	0.081	0.16	0.24	0.18	0.10	0.16	0.054

**Fig. 5** The Voronoi-diagram  $V_p(2, 3)$  in the Hammer-Aitof projection at  $cz = 7201$  Km/sec.

where  $\lambda$  is the intensity of the Poisson process. In our case  $\lambda$  is replaced by the random points. Our values of  $\bar{A}$ , see captions in Figure 4, are near to the values predicted by the mathematical theory. In order to obtain the number of edges/crossed faces we report in Table 1 the probability to have  $n$  edges for random seeds and the theoretical value as given in Okabe et al. (1992). The derived values of  $c$  remember the theoretical distribution of 1D Voronoi segments in which  $c=2$ , see Kiang (1966) .

### 3.2 Projection on the sphere

Another way to look at the cross sectional area is a spherical cut characterised by a constant value of the distance to the center of the box , in this case expressed in  $cz$  units, see Figure 5 .

### 3.3 The statistics of the volume

In every point-lattice  $L_{k,m,n}$  we compute the nearest seed and we increase by one the volume of that seed. The frequency histogram and the relative best fit through gamma-variate pdf for the volume distribution is reported in Figure 6. The experimental frequencies are fitted by a gamma-variate with  $c = 5.5$  . This value of  $c$  should be compared with the value of 6 as deduced by Kiang (1966) and successively refined in 5.5 due to a change in the generator of random numbers ( Kiang (1990)) and with 5.78 as deduced by Kumar et al. (1992).



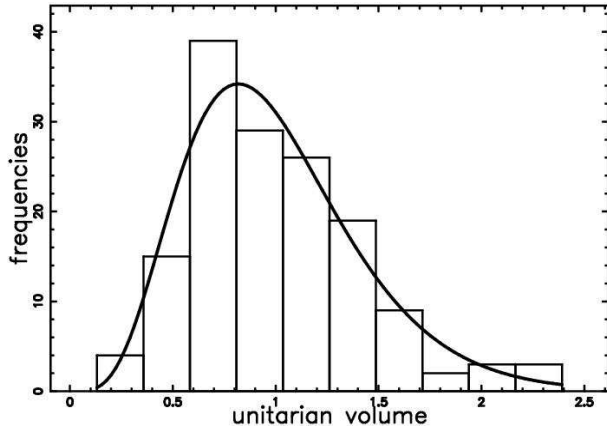


**Fig. 6** Histogram (step-diagram) of volume distribution with a superposition of the fitting line (the gamma-variate). Parameters as in Figure 3 but  $pixels = 400$  :  $c=5.50$ ,  $NBIN=10$  and  $\chi^2=8.05$ .

## 4 THE SPATIAL DISTRIBUTION OF GALAXIES

The theory of the sectional area derived in Sec. 3.1 can be the framework that explains the existence of voids in the spatial distribution of galaxies. The observational material that proves the existence of voids in the distribution of galaxies is briefly reviewed and then the number of voids in the distribution of galaxies that characterises the CFA2 slices is derived. The calibration of the Voronoi diagrams on the void of largest area measurable on the CFA slices allows to simulate the maximum in the galaxy's concentration present in the various type of slices versus  $cz$  and the 128 Mpc regularity.

### 4.1 The CFA2 slices

The second CFA2 redshift Survey, started in 1984, produced slices showing that the spatial distribution of galaxies is not random but distributed on filaments that represent the 2D projection of 3D bubbles. We recall that a slice comprises all the galaxies with magnitude  $m_b \leq 16.5$  in a strip of  $6^\circ$  wide and about  $130^\circ$  long. One of such slice (the so called first CFA strip) is visible at the following address <http://cfa-www.harvard.edu/~huchra/zcat/>; more details can be found in Geller & Huchra (1989). The already mentioned slice can be down-loaded from <http://cfa-www.harvard.edu/~huchra/zcat/n30.dat/>. The first of such slices presents many voids, the bigger one being  $4000 \div 5000$  Km/sec across (Huchra (2003)). The greatest possible attention should be paid to the derivation of the void with maximum area,  $A_{max}^{obs}$ , because is the area that allows the determination of the average extension of the voids in the distribution of galaxies. The average value of voids diameter can be derived

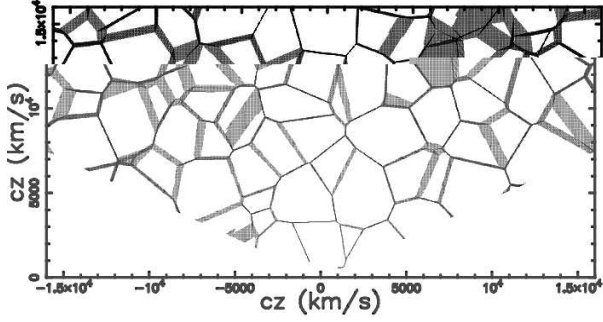


**Fig. 7** Polar plot of the little cubes belonging to a slice  $130^\circ$  long and  $6^\circ$  wide. Parameters as in Figure 3.

from the following proportion :

$$\frac{A_{max}}{\bar{A}} = \frac{A_{max}^{obs}}{\bar{A}^{obs}} \quad , \quad (7)$$

where the left hand side refers to the maximum and average value of the simulated cross-sectional area named  $V_p(2, 3)$  (their numerical values are visible in the captions of Figure 2) and the right hand side refers to the same quantities on the CFA2 slices. A value for the average observed diameter,  $\overline{D^{obs}}$ , is easily found from the previous proportion :

$$\overline{D^{obs}} \approx 0.6 D_{max}^{obs} = 2700 \frac{Km}{sec} = 27 Mpc \quad , \quad (8)$$

where  $D_{max}^{obs} = 4500 \frac{Km}{sec}$  corresponds to the extension of the maximum void visible on the CFA2 slices. The half value of  $\overline{D^{obs}}$  can be equated with equation 1 that gives the radius of the explosion from primeval galaxies and the following is obtained:

$$\frac{E_{64} t_9^2}{n-\gamma} = 1.47 \quad . \quad (9)$$

This relationship regulates the three basic physical parameters involved in the explosions of primeval galaxies.

The results of the simulation can be represented by a slice similar to that observed (a strip of  $6^\circ$  wide and about  $130^\circ$  long) , see Figure 7.

For a more accurate confrontation between simulation and observations the effect due to the distribution in luminosity should be introduced . Here conversely a "scaling" algorithm is adopted that is now summarised :

1. The field of velocity of the observed sample is divided in NBIN intervals equally spaced.
2. In each of these NBIN intervals the number of galaxies NGAL(j) , (j identifies the selected interval) , is computed.
3. The field of velocity of the simulated little cubes belonging to the faces is sampled as in point (1).

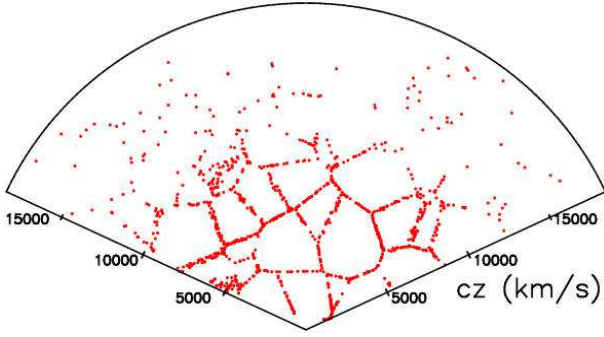


**Fig. 8** Polar plot of the little cubes (red points) when the "scaling" algorithm is applied. NBIN=15 and other parameters as in Figure 7 .

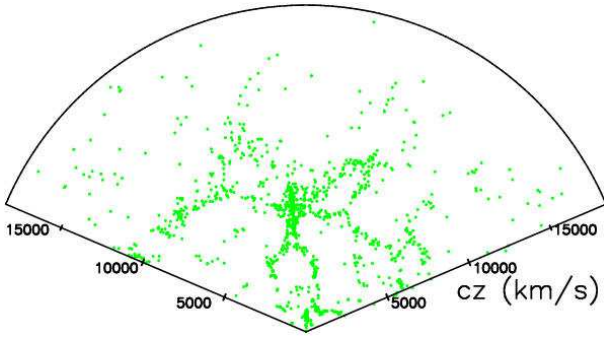


**Fig. 9** Polar plot of the real galaxies (green points) belonging to the second CFA2 redshift catalogue.

4. In each interval of the simulated field of velocity  $NGAL(j)$  elements are randomly selected .
5. At the end of this process the number of the little cubes belonging to the faces equalises the number and the scaling of the observed galaxies.

A typical polar plot once the "scaling" algorithm is implemented is reported in Figure 8; it should be compared with the observations , see Figure 9.

#### 4.1.1 The density of voids

The density of seeds expressed in physical units ,  $\rho_N$ , is the inverse of the physical averaged volume,  $\rho_N = \frac{1}{u_V^p}$ , and therefore

$$u_{A(2,3)}^p = (u_V^p)^{2/3} = \left(\frac{1}{\rho_N}\right)^{2/3} . \quad (10)$$

At the same time the sectional area will be characterised by a maximum physical area ,  $A_{max}^p$  expressed in physical units,

$$A_{max}^p = C_{Amax} \times u_{A(2,3)}^p \quad , \quad (11)$$

and the following is easily found

$$\rho_N = \left( \frac{C_{Amax}}{A_{max}^p} \right)^{3/2} \quad . \quad (12)$$

We are now ready to compute the number of sources in a sphere of radius  $R_{obs} = 16000 \text{ Km/sec}$  , the same radius that characterises the CFA2 slices. The number of voids/seeds in the sphere turns out to be

$$N = \frac{1.7 \cdot 10^{13} (C_{Amax})^{3/2}}{(A_{max}^{obs})^{3/2}} \quad , \quad (13)$$

where  $A_{max}^p$  was identified with  $A_{max}^{obs}$ . Inserting the dimension of the maximum void as deduced in §. 4.1, we obtain  $A_{max}^{obs} = 1.59 \cdot 10^7 (\text{Km/sec})^2$ . We now have an expression for the number of seeds in the sphere that characterises the CFA2

$$N = 268 (C_{Amax})^{3/2} = 827 \quad . \quad (14)$$

## 5 CONCLUSIONS

The Voronoi diagrams explain and characterise the voids in the spatial distribution of galaxies. The characteristics of a typical cell in a two-dimensional section of a 3D Voronoi diagram can be compared with those connected with the voids in the distribution of galaxies. The following items turn out to be useful to the astronomer once  $A_{max}^{obs}$  , the maximum area connected with a void, is derived from the astronomical slices:

- The averaged value of the voids in the distribution of galaxies should be  $2741 \pm 210$  Km/sec across.
- The pdf of the area of the voids in the distribution of galaxies should be a gamma-variate with argument 1.9.
- The expected averaged value of the sides of the irregular polygons that characterises the voids in the distribution of galaxies should be 5 .

Some important key questions are tentatively addressed to the astronomical community:

- The maximum area connected with a void should be derived with a great accuracy in the various slices.
- The algorithms of describing polygonal voids from the astronomical observations should be developed in order to test the suggested averaged number of sides, 5 , as predicted from the Voronoi diagrams.

- The pdf of the area connected with the voids should be tentatively computed in order to test the goodness of the  $V_p(2, 3)$  predictions.

The Voronoi diagrams allow also to reformulate the theory of the primordial explosions because

- The average diameter of voids between galaxies is function of three parameters : time , density and energy , see formula 9.
- The galaxies are originated where the primordial shells meet , the faces of the irregular polyhedra.
- The correlation length for galaxies can be identified with the face's thickness that is approximately  $\frac{1}{6}$  the radius of the expanding shell.

**Acknowledgements** I thank the Smithsonian Astrophysical Observatory and John Huchra for the small catalog available from the web at <http://cfa-www.harvard.edu/~huchra/zcat/>. I thank the referee for useful suggestions.

## References

- Barrow, J. D. & Coles, P. 1990, *Mont. Not. R. Astron. Soc.*, 244, 188
- Broadhurst, T. J., Ellis, R. S., Koo, D. C., & Szalay, A. S. 1990, *Nature*, 343, 726
- Charlton, J. C. & Schramm, D. N. 1986, *ApJ*, 310, 26
- Coles, P. 1991, *Nature*, 349, 288
- de Lapparent, V., Geller, M. J., & Huchra, J. P. 1988, *ApJ*, 332, 44
- El-Ad, H. & Piran, T. 1997, *ApJ*, 491, 421
- Folkes, S., Ronen, S., Price, I., et al. 1999, *Mont. Not. R. Astron. Soc.*, 308, 459
- Geller, M. J. & Huchra, J. P. 1989, *Science*, 246, 897
- Huchra, J. P. 2003, *private communication*
- Icke, V. & van de Weygaert, R. 1987, *A&A*, 184, 16
- Kiang, T. 1966, *Zeitschrift fur Astrophysics*, 64, 433
- Kiang, T. 1990, *private communication*
- Kiang, T. 2003, *Chinese Journal of Astronomy and Astrophysics*, 3, 95
- Kiang, T., Wu, Y.-F., & Zhu, X.-F. 2004, *Chinese Journal of Astronomy and Astrophysics*, 4, 209
- Kumar, S., Kurtz, S. K., Banavar, J. R., & M.G., S. 1992, *Journal of Statistical Physics*, 67, 523
- Okabe, A., Boots, B., & Sugihara, K. 1992, *Spatial tessellations. Concepts and Applications of Voronoi diagrams* (Chichester, New York: Wiley)
- Pierre, M. 1990, *A&A*, 229, 7
- Press, W. H., Teukolsky, S. A., Vetterling, W. T., & Flannery, B. P. 1992, *Numerical recipes in FORTRAN. The art of scientific computing* (Cambridge: Cambridge University Press)

- Ramella, M., Boschin, W., Fadda, D., & Nonino, M. 2001, *A&A*, 368, 776
- Ratcliffe, A., Shanks, T., Broadbent, A., et al. 1996, *Mont. Not. R. Astron. Soc.*, 281, L47+
- Saar, E., Einasto, J., Toomet, O., et al. 2002, *A&A*, 393, 1
- Shectman, S. A., Landy, S. D., Oemler, A., et al. 1996, *ApJ*, 470, 172
- Sheth, R. K. & van de Weygaert, R. 2004, *Mont. Not. R. Astron. Soc.*, 350, 517
- Subba Rao, M. U. & Szalay, A. S. 1992, *ApJ*, 391, 483
- van de Weygaert, R. & Babul, A. 1994, *ApJ*, 425, L59
- Voronoi, G. 1908, *Z. Reine Angew. Math*, 134, 198
- Zaninetti, L. 1991, *A&A*, 246, 291
- Zaninetti, L. & Ferraro, M. 1990, *A&A*, 239, 1